Netherlands foundation for radio-astronomy

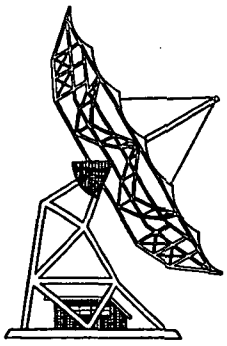

[redacted]

(NASA-CR-157920) MAPS OF JOVIAN RADIO EMISSION AT 1412 MHz Final Technical Report, 15 Jan. - 15 Oct. 1978 (Leiden Univ.) 28 p HC A03/MF A01 CSCL 03B G3/93 N79-11993 Unclas 36993

Stichting radiostraling van zon en melkweg

RADIOSTERRENWACHT DWINGELOO
Dwingeloo Nederland
Telefoon 05219-7244 - Telex 42043

RADIOSTERRENWACHT WESTERBORK
post Hooghalen Nederland
Telefoon 05939-421 - Telex 53621

I. INTRODUCTION

We observed Jupiter with the Westerbork Radio Telescope at a frequency of 1412 MHz in December 1977 when it was at its most northerly opposition to the earth. As was pointed out in Ch. III of the previous final technical report for grant NSG 7264 (hence forth referred to as Paper I) that was an optimal time to observe this planet.

We obtained pictures of Jupiter in all four Stokes parameters at 24 different rotational aspects of the planet, each integrated over 15 degrees of Jovian rotation. The maps clearly indicate the presence of higher order terms in the dipolar field of Jupiter at distances of $\sim$ 2 Rj from the center. They also show a displacement of the main dipole of 0.119 $\pm$ 0.009 Rj from the center of the disk towards longitude 135^{o}-145^{o} (Syst. III 1965.0) and a displacement of 0.04 $\pm$ 0.04 Rj towards the north in agreement with the displacement found by the Pioneer spacecrafts. From the data I would estimate the thermal disk temperature at this frequency to be more than 300 K but less than 340 K, which implies an ammonia mixing ratio of $\sim 5 \times 10^{-4}$ (Gulkis, 1973).

II. OBSERVING AND REDUCTION TECHNIQUE

The properties of the Westerbork telescope and its operation have been described extensively in Paper I. Since the circularly polarized flux of Jupiter can give much information concerning the magnetic field of the planet we tried to map this flux with an accuracy much better than generally obtained. Under normal circumstances the dipoles of the Western telescopes of the interferometers are aligned at position angle PA = 90^{o} and those of the Eastern telescopes at 45^{o} so they are "crossed" to each other (see

Fig. 1). If the dipoles are set parallel to each other it appears that we can map the circular polarized flux V with a much better accuracy, together with either U or Q depending on the position angles of the dipoles. Following the papers by Weiler (1973) and Weiler and Raimond (1976) we see that the complex outputs R of the four channels of an interferometer with the "crossed" configuration can be written as:

$$
\begin{aligned}
R_{xx} &= \frac{1}{2\sqrt{2}} G_{xx}(I\{1-\Delta_{xx}^{-}+i\theta_{xx}^{+}\}-Q\{1+\Delta_{xx}^{+}-i\theta_{xx}^{-}\} \\
&\quad +U\{1-\Delta_{xx}^{+}+i\theta_{xx}^{-}\}-iV\{1+\Delta_{xx}^{-}-i\theta_{xx}^{+}\}) \\
R_{xy} &= \frac{1}{2\sqrt{2}} G_{xy}(I\{1+\Delta_{xy}^{-}-i\theta_{xy}^{+}\}-Q\{1-\Delta_{xy}^{+}+i\theta_{xy}^{-}\} \\
&\quad -U\{1+\Delta_{xy}^{+}-i\theta_{xy}^{-}\}+iV\{1-\Delta_{xy}^{-}+i\theta_{xy}^{+}\}) \\
R_{yx} &= \frac{-1}{2\sqrt{2}} G_{yx}(I\{1+\Delta_{yx}^{-}-i\theta_{yx}^{+}\}+Q\{1-\Delta_{yx}^{+}+i\theta_{yx}^{-}\} \\
&\quad +U\{1+\Delta_{yx}^{+}-i\theta_{yx}^{-}\}+iV\{1-\Delta_{yx}^{-}+i\theta_{yx}^{+}\}) \\
R_{yy} &= \frac{1}{2\sqrt{2}} G_{yy}(I\{1-\Delta_{yy}^{-}+i\theta_{yy}^{+}\}+Q\{1+\Delta_{yy}^{+}-i\theta_{yy}^{-}\} \\
&\quad -U\{1-\Delta_{yy}^{+}+i\theta_{yy}^{-}\}-iV\{1+\Delta_{yy}^{-}-i\theta_{yy}^{+}\}).
\end{aligned}
\tag{3}
$$

where the G's are the complex instrumental gain factors, I, Q, U and V are the complex visibility functions of the four Stokes parameters. $\Delta^{-} = \Delta_W - \Delta_E$ are errors in the dipole setting of the Eastern and Western telescopes, i.e. an instrumental linear polarization, and $\theta^{+} = \theta_W + \theta_E$ represents an instrumental circular polarization. Both terms Δ and θ can be adjusted to a level of $\lesssim$ 1% of I. Neglecting these small terms in the

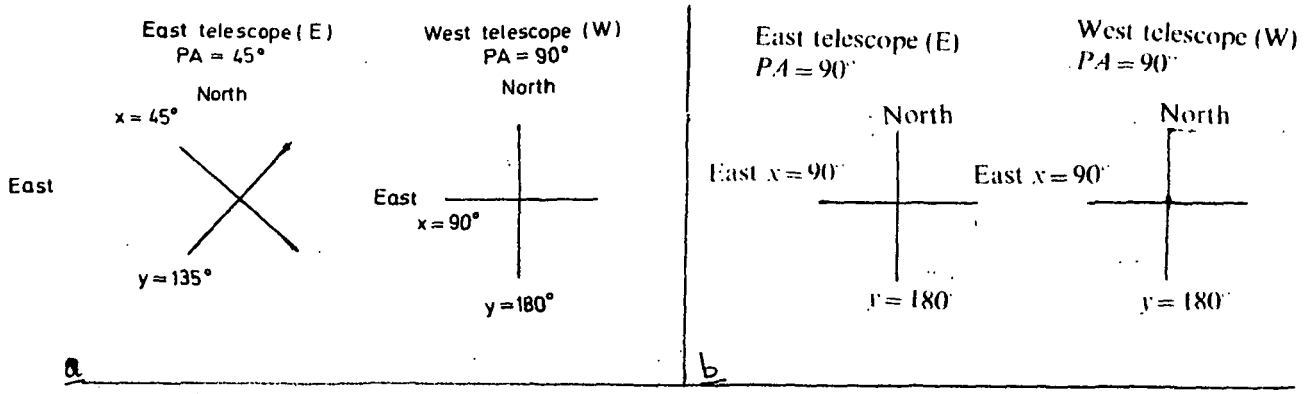

Fig. 1 Dipoles for the "crossed" resp. "parallel" configuration (from Weiler, 1973 and Weiler and Raimond, 1976). Each telescope has the two dipoles x and y.

solution for the four Stokes parameters cause errors of the order of 0.4% of I in the individual maps. Fluctuations in the system gains are of the order of $\lesssim$ 1% of the receiver output giving a total error of $\sim$ 0.5 % of I in all maps.

Setting the dipoles of all telescopes parallel to eachother at position angles 90° gives us the equations:

$$R'_{xx} = \tfrac{1}{2}G_{xx}\{I - Q - U(\Delta^{+}_{xx} - i\theta_{xx}) - iV(\Delta^{-}_{xx} - i\theta^{+}_{xx})\}$$
$$R'_{xy} = \tfrac{1}{2}G_{xy}\{I(\Delta_{xy} - i\theta^{+}_{xy}) + Q(\Delta^{+}_{xy} - i\theta_{xy}) - U + iV\}$$
$$R'_{yx} = -\tfrac{1}{2}G_{yx}\{I(\Delta^{-}_{yx} - i\theta^{+}_{yx}) - Q(\Delta^{+}_{yx} - i\theta^{-}_{yx}) + U + iV\}$$
$$R'_{yy} = \tfrac{1}{2}G_{yy}\{I + Q + U(\Delta^{+}_{yy} - i\theta^{-}_{yy}) - iV(\Delta^{-}_{yy} - i\theta^{+}_{yy})\}$$

Neglecting the terms (U, Q, V) (Δ, Θ) in this configuration cause errors of 0.1 % of I in the various maps and we can write the receiver output as:

$$R'_{xx} = \tfrac{1}{2}G_{xx}(I - Q)$$
$$R'_{xy} = \tfrac{1}{2}G_{xy}(I\varepsilon_{xy} - U + iV)$$
$$R'_{yx} = -\tfrac{1}{2}G_{yx}(I\varepsilon_{yx} + U + iV)$$
$$R'_{yy} = \tfrac{1}{2}G_{yy}(I + Q).$$

where $\varepsilon = (\Delta^- - \Theta^+)$, a complex instrumental error which can be found from calibration measurements as will be shown below. Together with the fact that possible gain fluctuations in the system are $\lesssim$ 1% of the receiver signals it will be clear that the disturbances in U and V generated by system errors causing "leakage" of I will be $\sim$ 0.1 % of I or less. 12 hr observations of the planet were made on each of five consecutive days in order to get finally two dimensional pictures of Jupiter at all rotational aspects, smeared over only 15^o of central meridian longitude (Dec. 16 - 21, 1977; one extra observation of 7^{hr} was made on the first day). To be able to calibrate the data we chose an observing sequence as listed in Table I. with the calibration sources shown in Table II.

After all measurements were corrected for known instrumental and sky effects (Paper I and van Someren Greve, 1974) we used the adopted flux of 3C147 to define the gain of the system assuming zero polarization for this source. The other three sources listed were used as geometry and phase calibrators. The complex correction factors G_{xx} and G_{yy} could be determined directly from the calibrations taken in the "parallel" configuration. However, we

Table 1: Observing sequence in December 1977

Sidereal day	Source	Observation time in min.	dipole configuration
350	3C48	40	x+
	3C286	15	x+
351	3C147	20	++
	Jupiter 1	7hr 1 min	|
	3C286	30	|
	3C48	40	|
	3C147	22	|
352	Jupiter 2	12hr 4 min	|
	3C286	60	|
	3C309.1	60	|
	3C48	220	|
	3C147	22	|
353	Jupiter 3	12hr 4 min	|
	3C286	7hr 12min	|
	3C309.1	83	|
	3C48	139	|
	3C147	20	|
354	Jupiter 4	12hr 4 min	|
	3C286	60	|
	3C48	45	|
	3C147	20	|
355	Jupiter 5	12hr 4 min	|
	3C286	60	|
	3C48	25	|
	3C147	20	|
356	Jupiter 6	12hr 4 min	|
	3C286	60	++
	3C286	60	x+
	3C48	40	|
357	3C147	120	|
	3C48	120	|
	3C147	90	|
	3C48	135	|
	3C286	83	x+

Table II: Calibration sources. The flux densities of 3C48, 3C286 and 3C309.1 are "mean" flux densities, derived from ratios to the flux density of 3C147.

Source	RA	Dec	Flux (21 cm)
3C147	84.68126	49.82858	21.57
3C48	23.70761	32.90573	(15.67)
3C286	202.20689	30.76633	(14.30)
3C309.1	224.73602	71.86977	(7.88)

are left with two unknowns in both the R'_{xy} and R'_{yx}. Using the calibration observations taken with the "crossed" configuration we were able to define the G_{xy} and G_{yx} for each observation due to the fact that the mutual channels of one interferometer are very stable (fluctuations are less than 1% in amplitude, and $0^{\circ}.5$ in phase). The observations of the unpolarized source 3C147 provided the complex instrumental error terms ε_{xy} and ε_{yx}. The Fourier components for each interferometer of the four Stokes parameters can then be represented by:

$$I = \tfrac{1}{2}(xx + yy) \qquad Q = \tfrac{1}{2}(yy - xx)$$

$$U = \tfrac{1}{4}\{-2xy + 2yx + (\varepsilon_{xy} - \varepsilon_{yx})xx + (\varepsilon_{xy} - \varepsilon_{yx})yy\}$$

$$V = -\frac{i}{4}\{2xy + 2yx - (\varepsilon_{xy} + \varepsilon_{yx})xx - (\varepsilon_{xy} + \varepsilon_{yx})yy\}$$

where xx, xy, yx and yy are the calibrated complex receiver outputs. It appeared that the maximum circular polarized intensities detected in the measurements of 3C286 and 3C48 was less than 0.1% of the maximum intensities of I; thus the instrumental error in the V maps indeed is less than 0.1% of I. The degree of linear polarization of 3C286 is 9.4 ± 0.05 % at an angle of 117°. These angles are not corrected for Faraday rotation in the earth's ionosphere which will cause errors of less than $\sim 5^{\circ}$ (Weiler and Raimond, 1976). The polarization of 3C286 is in excellent agreement with the numbers published by Berge and Seielstad (1972) ($P_L = 9.36 \pm 0.07$, PA = 32 ± 1.1) and Morris and Berge (1964) (P_L = 9.3 ± 9.5; PA = 32 ± 2); the first publication yield numbers for 3C48 of P_L = 0.43 ± 0.07, PA = 139.7 ± 4.8, the second one of P_L = 0.6 ± 0.6, 0.7 ± 0.6 and PA = 154 ± 28, 162 ± 25. Morris and Berge (1964) also measured 3C147 to have a P_L of 0.6 ± 0.3 and 0.2 ± 0.5 with

PA = 173 $\pm$ 10, 138 $\pm$ 57. The position angles are not corrected for Faraday rotation in the earth's conosphere. Since observations of 3C147 and 3C48 show very small values for the degree of linear polarization it will be clear that these numbers and in particular the position angles largely depend on the "chosen" polarization of the calibration source.

At its time of observation Jupiter was at a distance of 4.1525 AU from the earth, so that the measured flux densities were multiplied by a factor of $(\frac{4.1525}{4.04})^2$ to correct them to those at the standard distance of 4.04 AU.

After removing the effect of the planetary motion along the sky from the Jovian data (as we did in Paper I), we cut the observations into 25 min. pieces, which is about 15^o of Jovian longitude. This creates a smearing effect on the data which amounts to $\sim$ 20 arcsec at an angular distance of $\sim$ 3 Rj.

Fig. 2 shows very schematically the coverage of the UV plane for these data together with a picture of the beam with which we have "observed" the planet. Compared to the 1973 data presented in Paper I, we now have a much better coverage of the UV plane (6 observations equally spread in hour angle) and much less trouble with the quality of the calibration since the planet was at a much higher declination and thus elevation.

Using the procedure called CLEAN, the deconvolution technique developed by Högbom (1974) we were able to remove the antenna pattern from the maps so that after having restored the components to the map using a Gaussian shaped beam (with a half power width of 16".6) the uncertainties in the maps appeared to be $\sim$ 1% of the maximum intensity

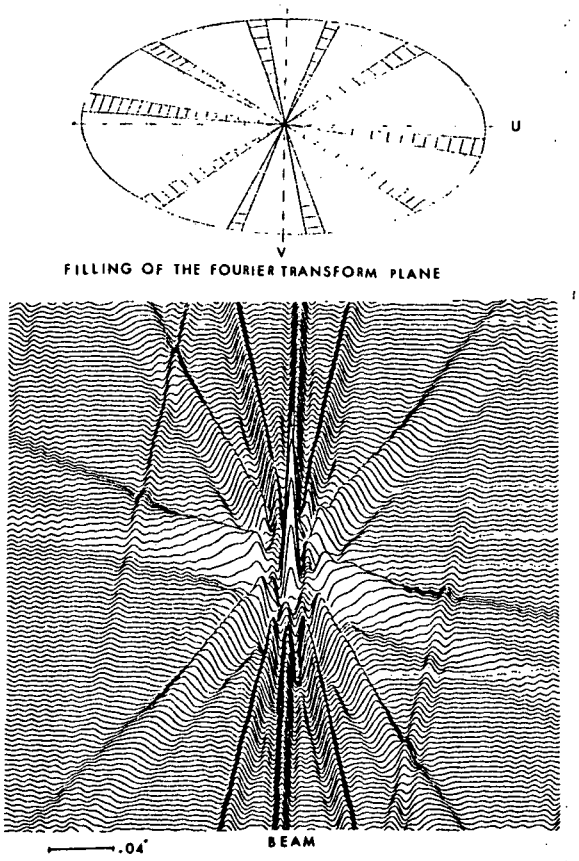

Fig. 2 The upper part of the figure shows very schematically the filling of the Fourier transform (UV) plane used to map Jupiter at all rotational aspects of the planet. The lower part shows the beam with which we are looking at the planet at a particular longitude.

in the I maps, 1.5 - 2.0% of the maximum response in the polarized ($\sqrt{Q^2+U^2}$) maps, and the V maps were accurate to 0.1% of the maximum intensities of the I maps. The position angles were corrected for Faraday rotation in the ionosphere using electron density data obtained from the Dutch meteorological Institute in the Bilt, which gave a correction of $1^{\circ}.43$ with variations up to 20 - 30%. The error remaining in the position angles is $\sim 0^{\circ}.5$.

III. INTEGRATED JOVIAN PARAMETERS

Fig. 3 and 4 show various parameters of the integrated Jovian radiation as functions of, respectively, Jovian magnetic longitude (Syst. III 1965.0) and magnetic latitude of the earth with respect to Jupiter. The parameters are calculated by integrating the two-dimensional Jovian maps in I, Q, U and V, which all are averaged over 15^{o} intervals.

Indicated are:

a the total integrated flux density in Jy

b polarization direction: the position angle of the electric vector measured eastward from the north in the sky (corrected for Faraday rotation in the earth's ionosphere, see Section II)

c degree of linear polarization

d degree of circular polarization

e (in Fig. 3) the magnetic latitude of the earth with respect to Jupiter. This latitude was calculated according to $\theta_m = D_E + \beta \cos (l_{III} - l_o)$ (as in Paper I). D_E is the declination of the earth relative to Jupiter's rotational equator ($+ 2^{o}.24$ at this epoch), β is the angle between Jupiter's magnetic and rotational axes taken as 10^{o} and l_o is the central meridian longitude of the magnetic north pole taken as 201^{o} (as in Paper I).

The variations with longitude are consistent with the beaming found by others from the integrated data (see Paper I). Since the present observations were made in an epoch when the declination of the earth D_E was positive we find a much deeper minimum at $l \sim 200^{o}$ than at $l \sim 20^{o}$. Again the maximum in S at ~ 300 is higher than at $\sim 100^{o}$. With the help of the data shown in this paper we can interpret this difference as being caused by the presence of a region of enhanced emissivity near $l \sim 250^{o}$ (as was already suggested by de Pater and Dames, 1978) together with the fact that the magnetic field has

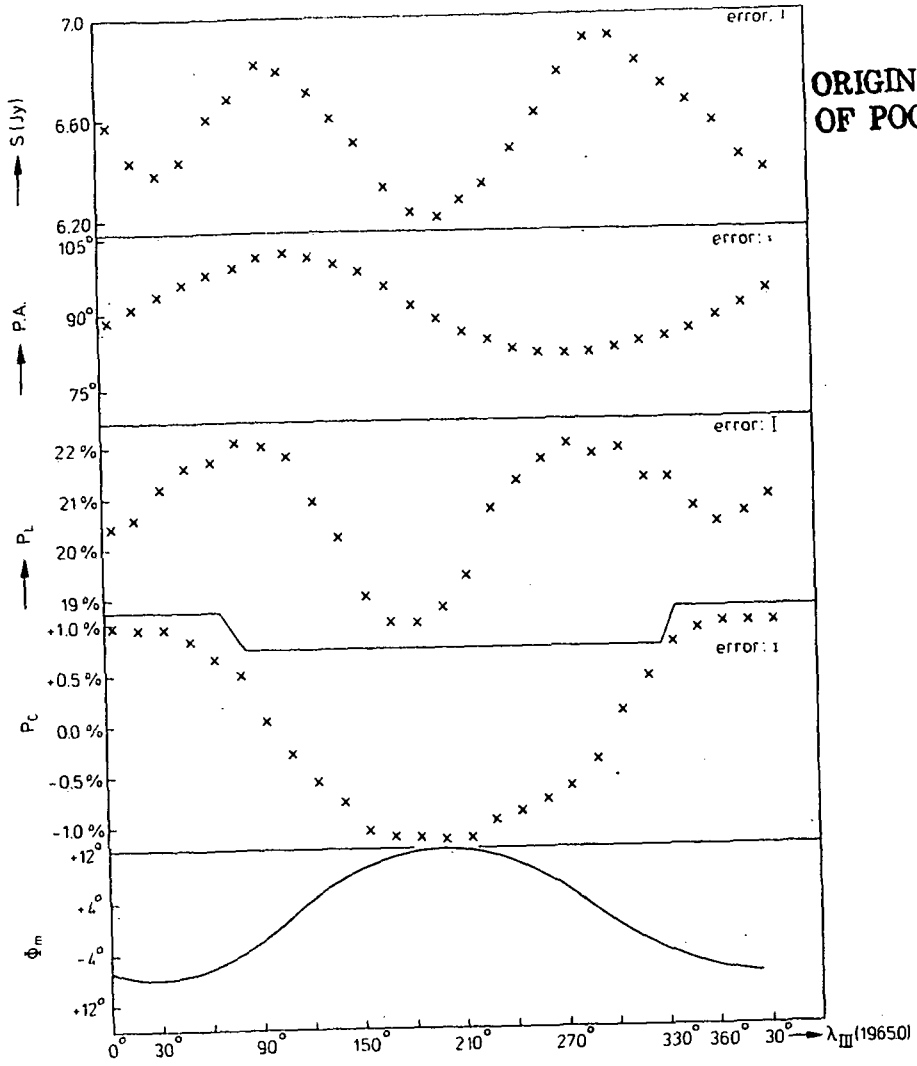

ORIGINAL PAGE IS
OF POOR QUALITY

Fig. 3 Various parameters of the integrated radiation from Jupiter at 21cm as functions of the magnetic longitude of Jupiter (in Syst III 1965.0)

a) integrated flux density in Jy

b) position angle of the electric vector measured earthward from north in the sky

c) degree of linear polarization

d) degree of circular polarization

e) magnetic latitude of the earth with respect to Jupiter.

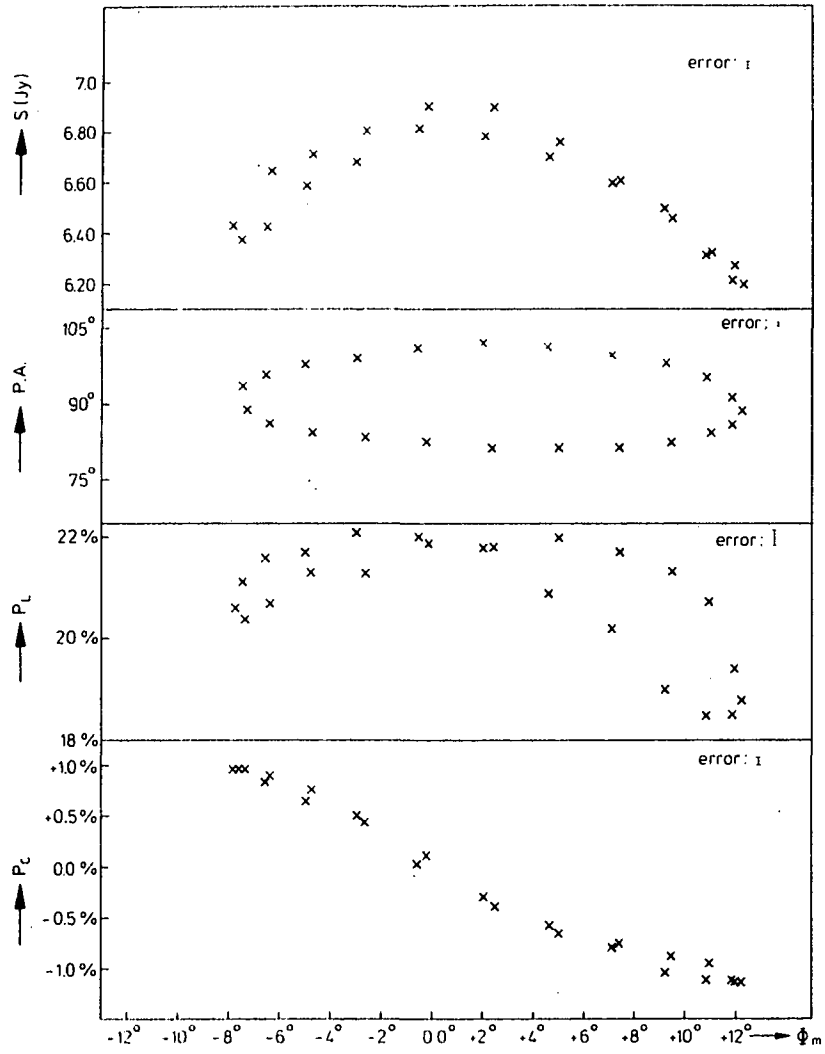

Fig. 4 The parameters a-d from Fig. 2 are plotted as functions of the magnetic latitude of the earth with respect to Jupiter.

a multipole character rather than a dipolar one at $\sim$ 2 Rj from the center (see section IV). The degree of circular polarization in Fig. 2 clearly shows maxima at the longitudes of the magnetic poles with a slightly higher maximum at 1 $\sim$ 200^{o} caused by the positive declination D_E. The curve however shows a rather large deviation from a pure sine curve, which is pronounced in Fig. 4 by the flattening of the curve at the ends of ϕ_m. This flattening is determined by the pitch angle distribution of the electrons (Roberts and Komosaroff, 1976), which in general can be written as $\Sigma\ \Delta_q\ \sin^q \alpha_e$, where α_e is the equatorial pitch angle. When q = 0 the distribution is isotropic, larger values of q specify flatter pitch angle distributions. Roberts and Komosaroff (1976) point out that to fit the beaming of the radiation and the curves for linear and circular polarization for their data they need a $q_1 = 1$ and $q_2 \gtrsim 30$.

IV. TWO-DIMENSIONAL JOVIAN MAPS

Fig. 5 shows the two-dimensional maps of Jupiter at 21 cm at all rotational aspects of the planet averaged over 15^{o} of Jovian central meridian longitude. Indicated are maps of the total intensity, circular and linear polarized flux and the magnetic field of the planet. This last map is made by rotating plots of the position angle of the electric vector (corrected for Faraday rotation in the earth's ionosphere as mentioned in section II) over an angle of 90^{o}. It is assumed herewith that there is no Faraday rotation within Jupiter's magnetic field, a generally accepted idea which was confirmed in Paper I considering the integrated parameters of the source of λ = 21 cm and λ = 50 cm. For individual parts of the source we can write the rotation measure R_m as: $R_m = 2.62 \times 10^{-17} \int n_e . \underline{H} . dl$ where R_m is in radians/$_{cm}2$, n_e is the number of thermal electrons/$_{cm}3$ (50-100/cm^3 , Intrilligator and Wolfe,

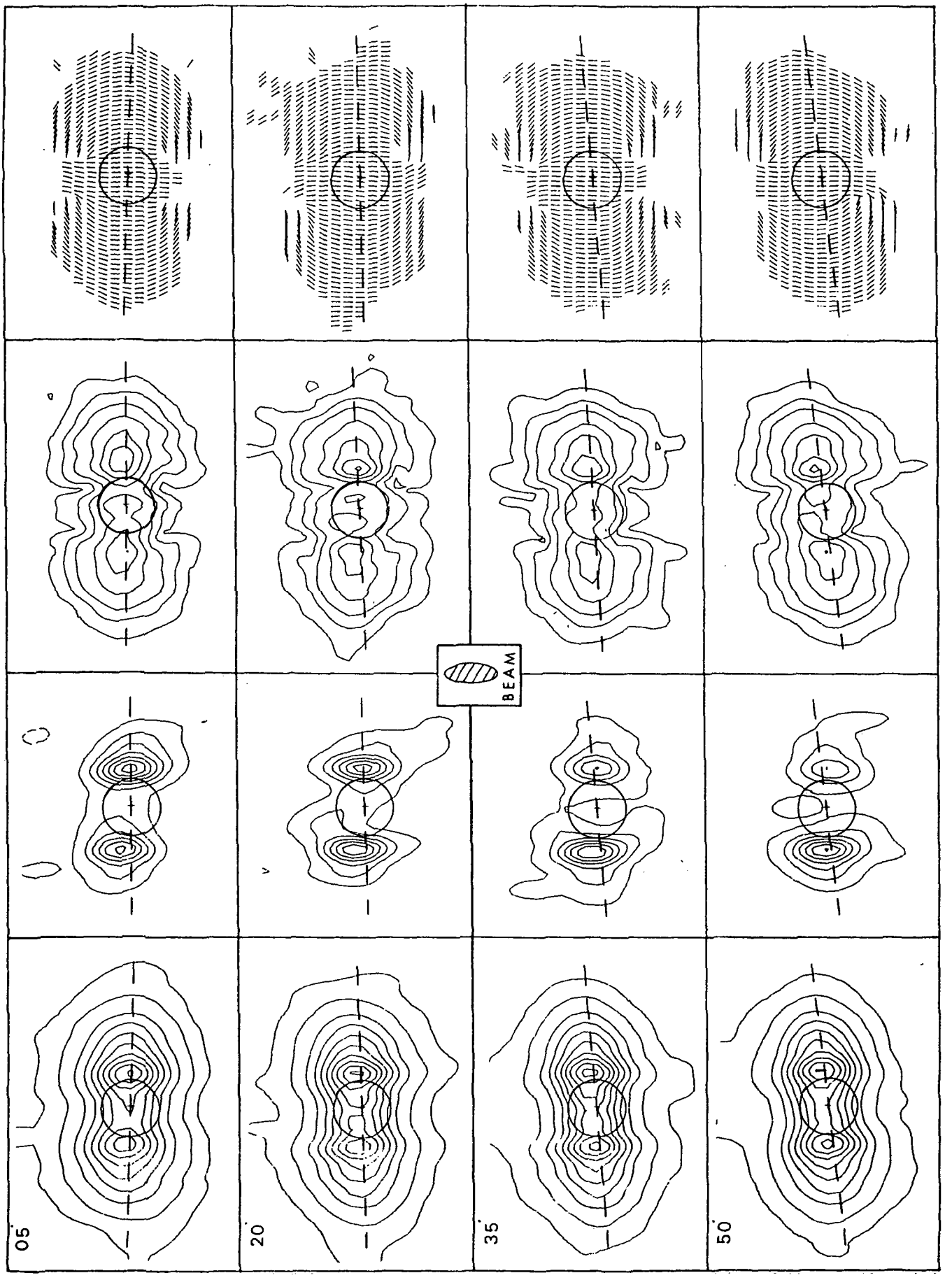

Fig.5a

ORIGINAL PAGE IS
OF POOR QUALITY

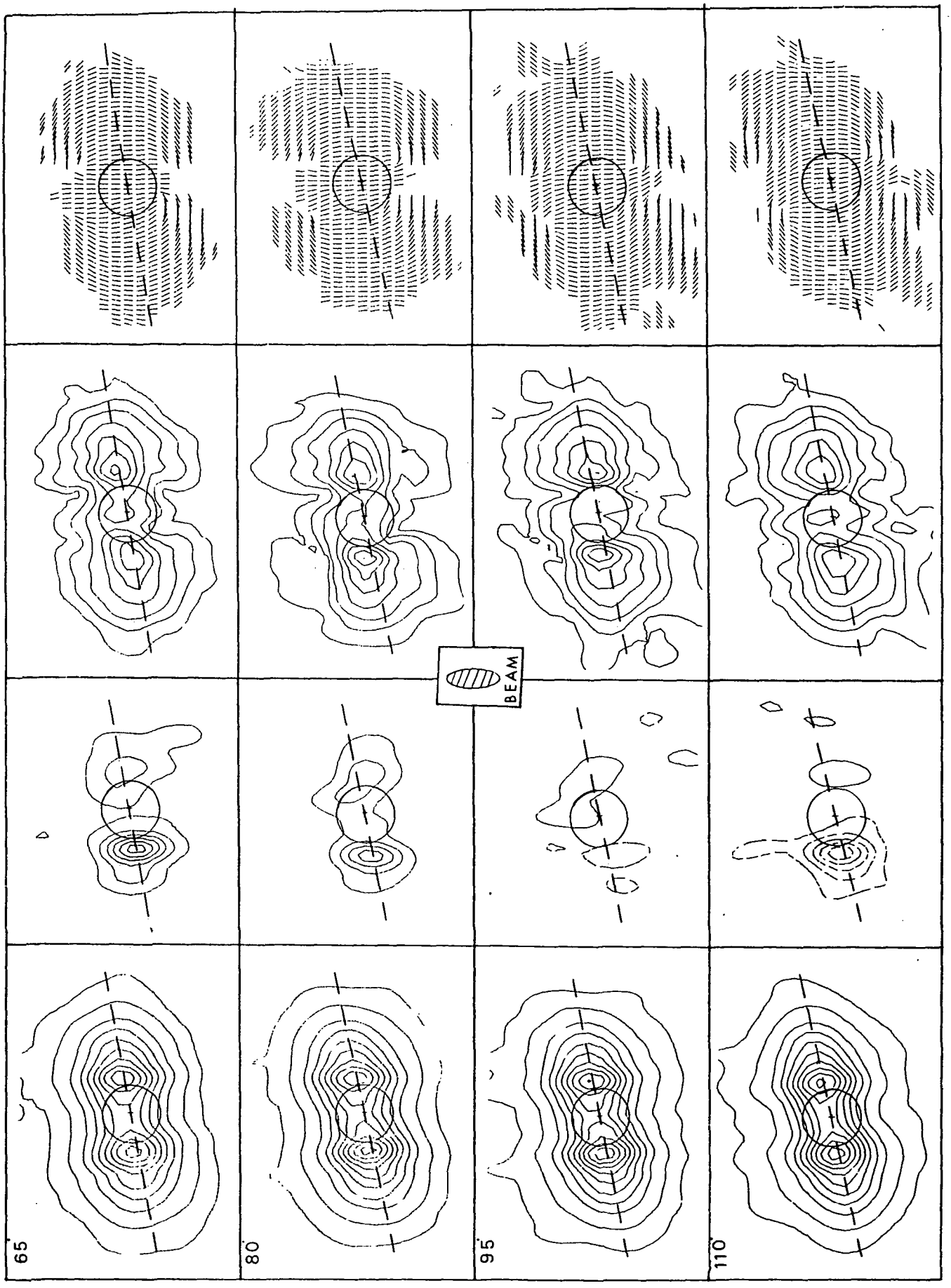

Fig. 5b

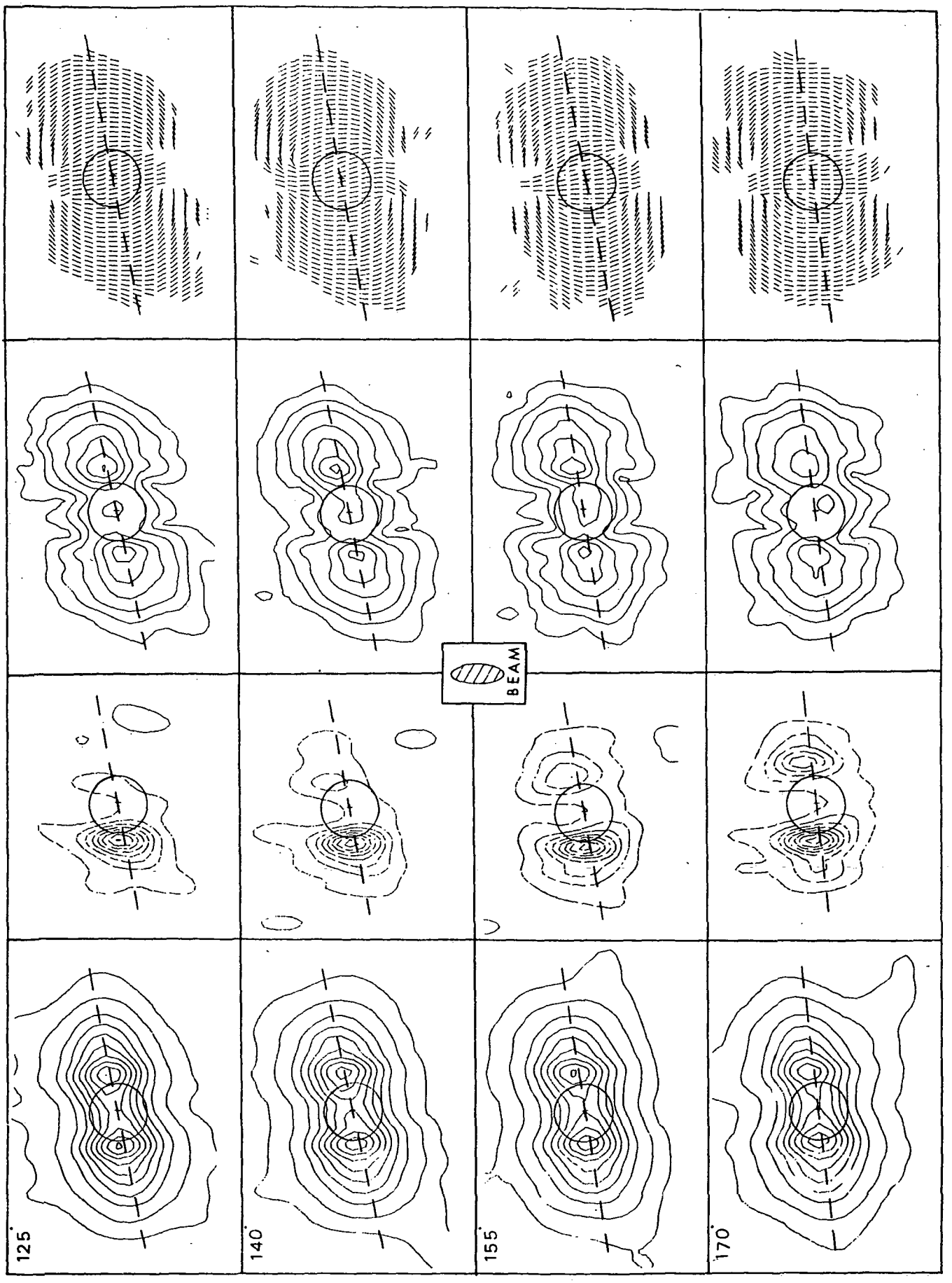

Fig.5c

ORIGINAL PAGE IS
OF POOR QUALITY

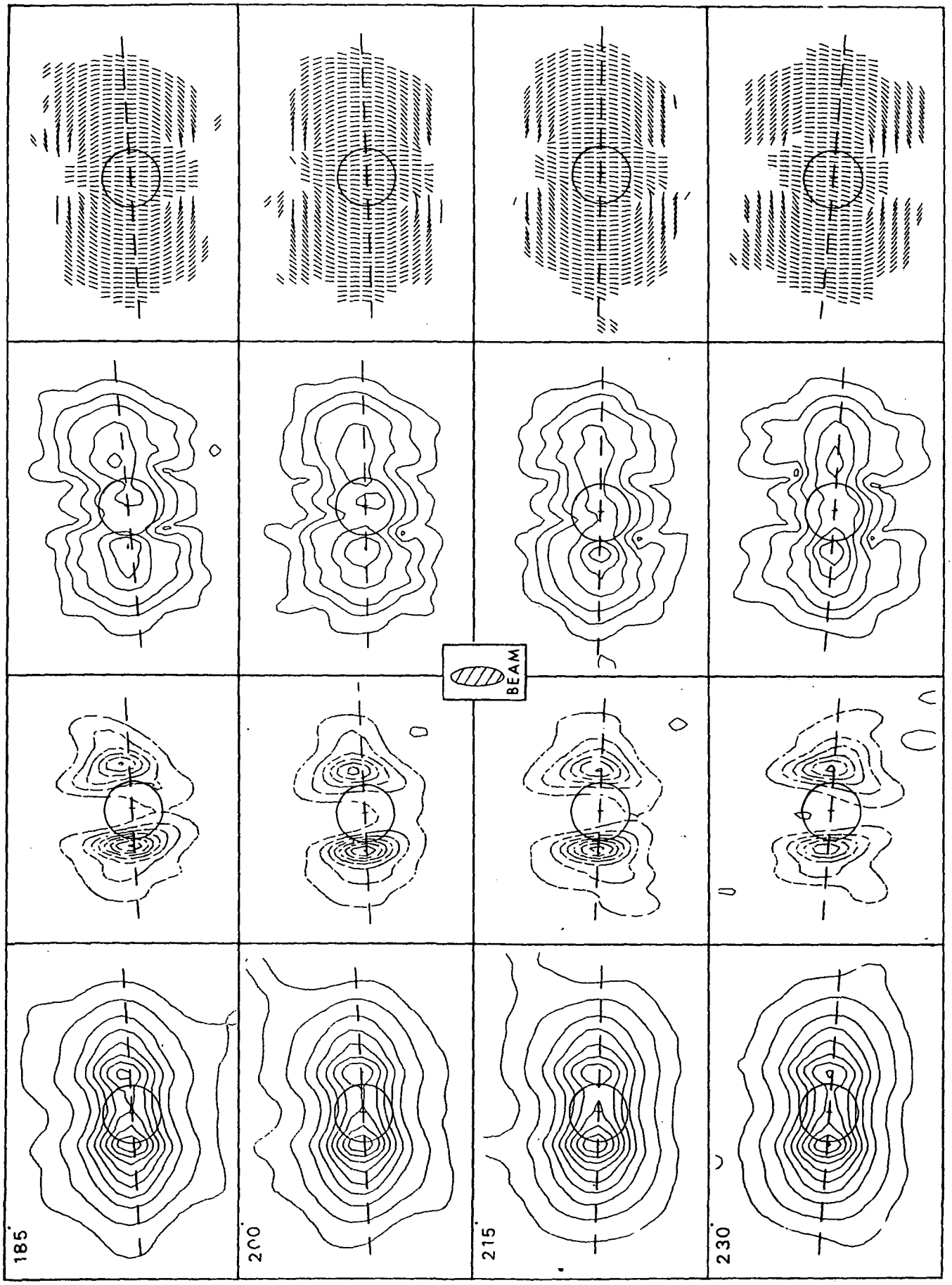

Fig.5d

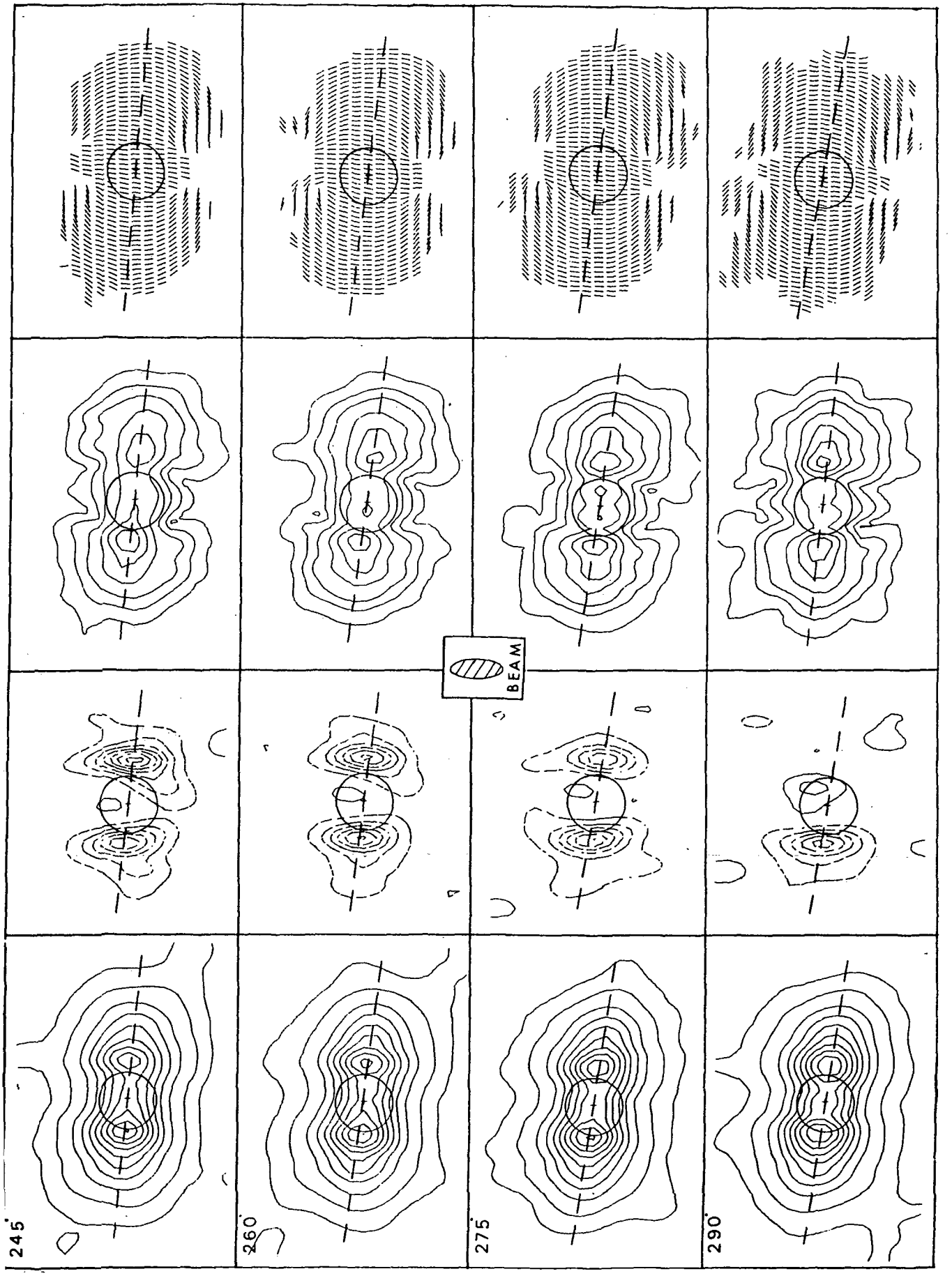

Fig.5e

ORIGINAL PAGE IS
OF POOR QUALITY

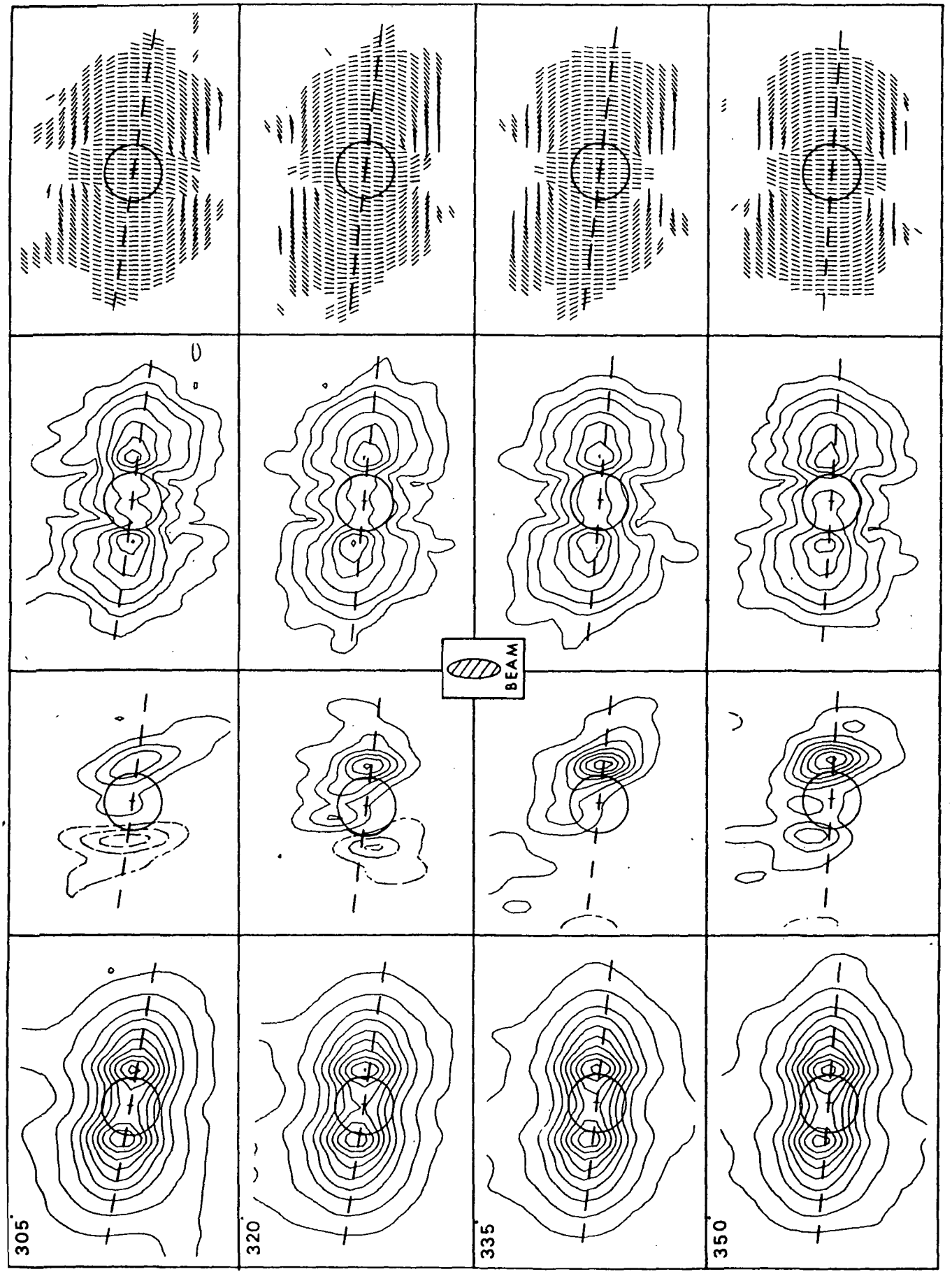

Fig.5f

1976 - but they point out that it is very difficult to measure this amount!) $\underline{H}$ the magnetic field strength along the line of sight in Gauss (exactly zero for a pure dipole field if you are in the equator!) and 1 the distance in cm. We see that the Faraday rotation $R_m\lambda^2$ near 1-2 Rj from the center at λ = 21 cm is less than $\sim 2^o$. The total intensity maps show the existence of a region of somewhat increased emission which we shall call a "hot" region, imbedded in the Jovian field at a longitude of $\sim 250^o$. However, at some longitudes where we expect to see this region at one side of the disk there is practically no difference in the amount of flux received from both sides of the disk - see f.e. the maps at $l_{III} \sim 110^o$; 125^o. This same feature is shown in the maps in paper I.

The maps of the circular polarized flux are not at all symmetric at these longitudes. In this report I assume that most electrons are near the magnetic equator with pitch angles near 90^o. In the future I will find out whether it is possible to get changes in this distribution at places where the field is distorted and whether or not a change will influence our model. The circularly polarized flux is a measure of the magnetic field component directed along the line of sight. Its intensity is related to the square root of the strength of the field along this direction and its sign shows whether the field is directed towards us (left handed polarization $\sim$ negative sign) or away from us (right handed polarization $\sim$ positive sign). We therefore tried to roughly interpret Jupiter's magnetic field with help of these maps of the circular polarization and the total intensity. In Fig. 6 I plotted the maximum amount of circularly polarized flux received within a square of 158 arcsec^2 for the left side of the belt as a function of magnetic longitude (6a) together with the maximum intensity from that side (6b). Taking a model for the radiation belt as shown at the right side with a region of enhanced

emissivity of 11-12% at $\sim 250^{o}$ with a sign of $\sim 80^{o}$ in longitudes centered at $l_{III} \sim 250^{o}$ of $\sim$ 11-12% we can predict the variation with longitude of both kinds of observed flux density. The sinusoid expected for the circular flux is sketched with a thin line in Fig. 6a; the dotted curve in b shows the variation in flux expected from only a rotating "hot region" in the field; modifying this curve with the sinusoidal variation as expected from the beaming caused by the wobbling of the equator gives us the thin curve drawn in b. Large deviations between the observed and expected curves

Fig. 5 Two dimensional maps of Jupiter: indicated are from left to right maps of the total intensity, circular and linear polarized flux and a vector diagram of the magnetic field of Jupiter (see text). The magnetic longitude of the central meridian (Syst. III 1965.0) is indicated in the upper left corner of each serie of 4. The contour values in mJy/beam are:

I : 7.5 (lower contour); 50-950 in steps of 100

V : 1.50-21.75 in steps of 2.25

P_L: 7.5 (lower contour), 25-350 in steps of 50.

The beam area is 18.093 points. The grid point spacing is 4".186 (= 0.177 Rj) in RA and 10".636 in Dec. The magnetic equator and planetary disk are indicated in the pictures.

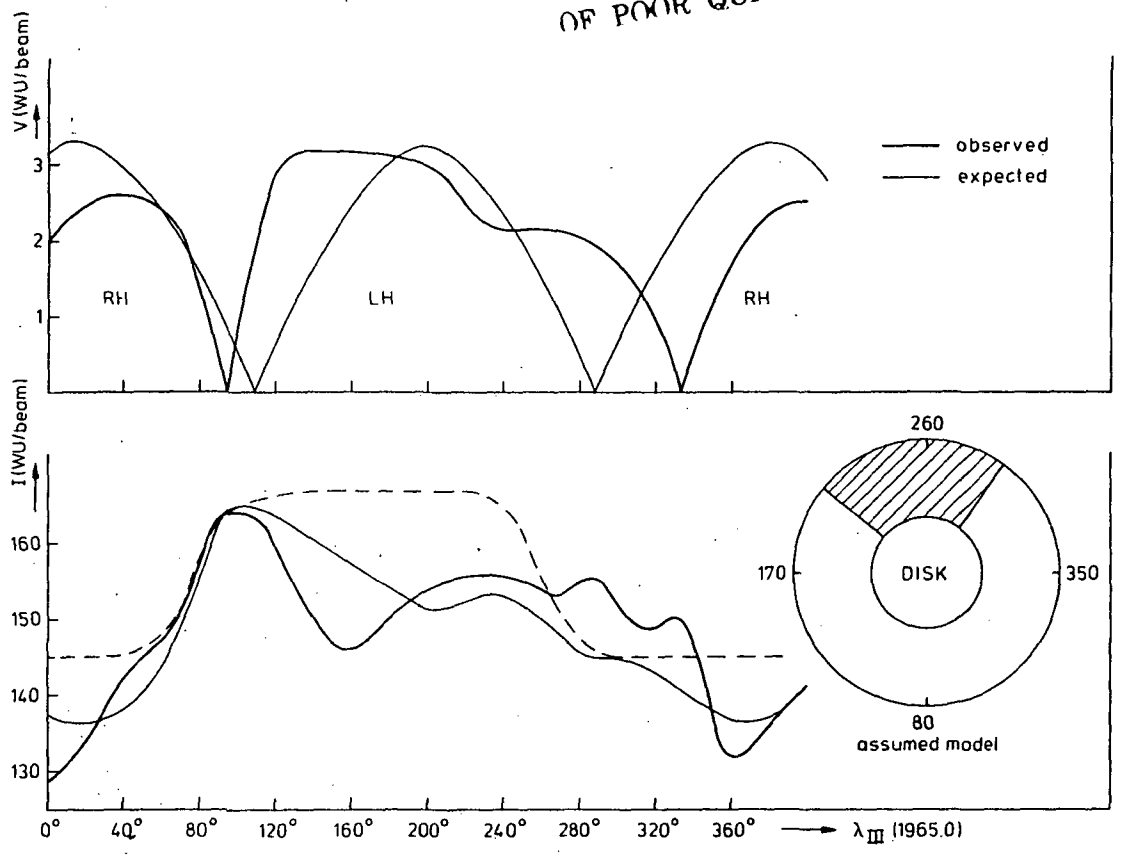

Fig. 6 In the upper part the mean maximum amount of circular polarized flux received within a square of 3x3 gridpoints at the leftside of the belt is plotted as a function of magnetic longitude (thick line), together with a sinusoid expected for a simple rotating dipole field (thin line). The lower part shows the maximum intensity at that side of the belt (thick line) together with the expected curve based on the model shown at the right side (for more details the reader is referred to the text).

The numbers indicated on the right side are in units of 5 mJy/beam.

show up, e.g. the distance of $\sim 240^{o}$ rather than 180^{o} between the longitudes of the zero values of the circularly polarized flux and the rather sharp increase in V and decrease in I near $1 \sim 100^{o}$-160^{o}. The fact that the circularly polarized flux increases much faster than expected indicates that, at that location, the magnetic equator is directed downwards with respect to the line of sight as if we are looking at the longitude of the north magnetic pole. Modifying our sinusoidal beaming curve in I in that manner will diminish the discrepancy between both curves drawn there.

CONCLUSION

Both plots clearly show that the magnetic equator whobbles in a non-dipolar way and we have to compare our maps with multipole models. In a first approximation I took the model of Smith et al. (1976) based on Pioneer 11 data to compare with our data. This model consists of a series of spherical harmonics; the quadrupole and octupole terms cause deviations from a pure dipole model with the largest anomalies near longitudes $\sim 50^{o} + n.90^{o}$.

Taking into account a region of enhanced emissivity at $\lambda \sim 200^{o}$-300^{o}, (where the gradient in the magnetic field is rather small) Smith's model gives rather good qualitative agreement between the variation with longitude of the circular polarized flux and the difference in this flux between both sides of the belt. The appropriateness of such a model to match the radio data was first suggested by E.Gerard (1976).

In the next one or two years I will develop more detailed multipole magnetic field models and I hope to finally get a three-dimensional model of the field coupled with an electron and pitch angle distribution in that field. Knowing the field structure and particle distribution one

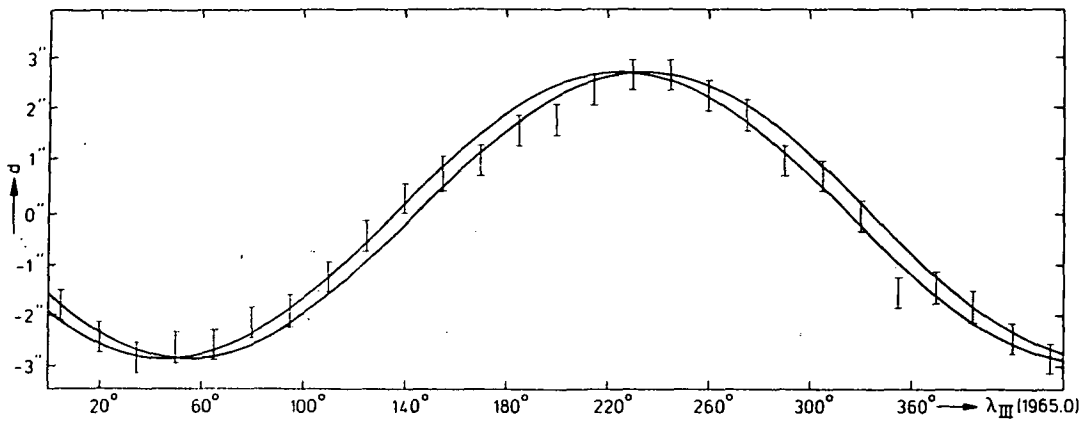

Fig. 7 The distance of the centre of the dipole field of Jupiter from the centrum of the optical disk are shown as a function of magnetic longitude. This distance is measured along the magnetic equator, positive towards the right (decreasing R.A.).

can define the thermal disk temperature with much better accuracy by the two different methods described in paper I.
Estimating this temperature from the maps shown in Fig. 5 with a "mean" dipolar field model for Jupiter, we find a temperature more than $\sim$300 K but less than $\sim$340 K. This implies a mixing ratio for ammonia (see Paper I) of $\sim 5 \times 10^{-4}$.

Fig. 7 shows a graph of the center of the dipole field of Jupiter as a function of the magnetic longitude. Since the higher order terms in the magnetic field decrease much faster going away from Jupiter (Quadrup $\sim r^{-4}$; Octupole $\sim r^{-5}$) than the (much larger) dipolar term we can approximate the field at $\sim$ 4-5 Rj as being dipolar. Taking the mean

position of this dipole field measured along the magnetic equator we find a deviation from the optical center of the planet as shown in Fig. 7. It appears that the dipole is displaced by 2".8 ± 0".2 or 0.119 ± 0.009 Rj towards a longitude of ∿ 135°-145°, which is in agreement with the displacement found by the Pioneer spacecrafts. A displacement of the dipole towards the north of 0.04 ± 0.04 Rj can be found from the maps, also in agreement with the Pioneer results.

V. SUMMARY

A preliminary interpretation of the Jovian observations from Dec. 1977 shows us:

a) the presence of higher order terms in the dipolar field of Jupiter at distances of ∿2 Rj from the center

b) confirmation of the hot region

c) a displacement of the main dipole from the center of the planet of 0.119 ± 0.009 Rj towards l ∿ 135°-145° and 0.04 ± 0.04 Rj towards the north, in agreement with the displacements the Pioneers found.

d) a thermal disk temperature at 21 cm of ∿ 300-340 K, implying a mixing ratio of ammonia in the Jovian atmosphere of ∿ 5×10^{-4}.

Acknowledgements. The observations for this joint NASA-Westerbork project were made at the Westerbork Radio Observatory. This institute is operated by the Netherlands foundation for Radio Astronomy with the financial support of the Netherlands organization for the advancement of Pure Research (Z.W.O.).

REFERENCES

Berge, G.L. and Seielstad, G.A., 1972: Astron. J. 77, 810

Gérard, E., 1976: Astron. & Astrophys., 50, 353.

Gulkis, S., 1973: Space Sci. Rev. 14, 497.

Högbom, J.A., 1974: Astron. & Astrophys. Suppl. 15, 417.

Intrilligator, D.S. and Wolfe, J.H., 1976: in Jupiter, Ed. T. Gehrels, University of Arizona Press. Tucson, Arizona, p.848.

Morris, D. and Berge, G.L., 1964: Astron. J. 69, 641.

de Pater, I. and Dames, H.A.C.. 1978: Astron. and Astrophys. in press.

Roberts, J.A. and Komesaroff, M.M., 1976: Icarus 29, 455.

Smith, E.J., Davis, L. Jr. and Jones, D.E., 1976: in Jupiter, Ed. T. Gehrels, University of Arizona Press, Tucson, Arizona, p.788.

van Someren Gréve, H.W., 1974: Astron. & Astrophys. Suppl. 15, 343.

Weiler, K.W., 1973: Astron. & Astrophys. 26, 403.

Weiler, K.W. and Raimond, E., 1976: Astron. & Astrophys. Suppl. 52, 397.